

Transition to spatially periodic patterns in nematics under oscillatory shear flow: linear analysis

O.S. Tarasov^{1,2}, A.P. Krehov^{1,2} and L. Kramer¹

¹*Institute of Physics, University of Bayreuth, D-95440 Bayreuth, Germany*

²*Institute of Molecule and Crystal Physics, Russian Academy of Sciences, 450025 Ufa, Russia*
(October 30, 2018)

We consider the orientational instabilities, both homogeneous and spatially periodic, developing in a nematic liquid crystal under rectilinear oscillatory Couette flow for director alignment perpendicular to the flow plane. Using numerical and analytical approaches we determine the critical amplitude of oscillatory flow instabilities, the critical wave number and the symmetry of the destabilizing mode. It was found, that by varying of the oscillatory flow frequency the instability changes its temporal symmetry. The mechanism of this transition is coupled with the inertia of the nematic fluid. We also shown that an electric field applied to the nematic layer can induce switching between instabilities with different spatial and temporal symmetries. The complete phase diagram of the flow instabilities is presented.

I. INTRODUCTION

Nematic liquid crystals (nematics) represent one of the simplest anisotropic fluid [1]. In order to describe the macroscopic dynamics of these materials made up from elongated molecules one introduces as additional hydrodynamic variable a unit vector \mathbf{n} , the *director*, which describes the axis of local preferred molecular orientation. The strong coupling between the director and velocity field provides a number of interesting phenomena in nematics under flow of different types, such as pattern formation [2,3], director tumbling [4], autowaves [3] *etc.*. The flow behavior of a nematic strongly depends on the geometry and material parameters, in particular the viscosity coefficients $\alpha_1 \dots \alpha_6$ known as Leslie coefficients. Two of these coefficients, α_2 and α_3 , appear in the director equation and play an particular role in hydrodynamic instabilities. α_2 is supposed to be negative for materials made of rod-like molecules, whereas the sign of α_2 is not restricted. If the nematic is initially oriented *within the flow plane* ($= x, z$ plane) then, in materials with $\alpha_3 < 0$ under steady flow (plane Couette or Poiseuille type) the director tends to align at an angle $\theta_{fl} = \tan^{-1} \sqrt{\alpha_3/\alpha_2}$ to the flow direction in the flow plane ($= x$ direction), which corresponds to stationary homogeneous solution of the nematodynamic equations [5]. Such nematics are called *flow-aligning*. The solution θ_{fl} with appropriate sign of the square root was shown to be linearly stable in the case of steady flows [5–7]. In oscillatory flows the director tends to oscillate between $\pm\theta_{fl}$. With a nonlinear velocity profile, as in Poiseuille flow, this solution can lose stability [8,9]. In the case $\alpha_3 > 0$ under steady flow one has tumbling with a director profile depending strongly on the shear rate [4]. Nematics with $\alpha_3 > 0$ are called *non-flow-aligning*. The picture of orientational transitions becomes even richer if the director is initially oriented *perpendicular to the flow plane* (y direction). This orientation corresponds, for symmetry reasons, to a stationary homogeneous solution of dynamic equations of nematics. With appropriate surface alignment it can lose stability at a certain magnitude of the shear rate via a stationary bifurcation [10,11]. In the absence of external fields in steady Couette as well as Poiseuille flows the director profile then deforms homogeneously in space. In steady Couette flow a magnetic field applied along the initial director orientation changes the type of instability from homogeneous to spatially periodic at a critical field strength [10]. In Poiseuille flow the magnetic field does not affect the type of instability [11], but rolls can be observed above a secondary instability [11]. Classical experiments of Pieranski and Guyon (PG) on oscillatory Couette flow [10] and recent experiments [12,13] show the appearance of a roll instability with the critical shear rate depending on flow frequency. It was shown by PG, that the temporal symmetry of the instability is influenced by an applied electric field [10]. A theoretical treatment of the problem [10,14,15,2] gives the mechanisms of the instability and is in a good agreement with experimental results, including the change in symmetry. For oscillatory Poiseuille flow the situation is similar [16–18]. In all the theoretical treatments [10,14–16,18] the inertia of the fluid is neglected, which is reasonable for the low frequencies used. In the absence of an electric field one then has no changes in the stability scenario as a function of the flow frequency.

In the present work we investigate numerically as well as analytically orientational instabilities, both homogeneous and spatially periodic, induced by plane, oscillatory Couette flow in nematics in the geometry with the director

pre-aligned *perpendicular to the flow plane* in a wide range of the flow frequencies. We look for homogeneous and spatially periodic instabilities and study the influence of an electric field on flow instabilities for both, negative and positive, dielectric anisotropy of nematic. Recent experiments [12,13] show that high-frequency range could also be investigated experimentally as well.

II. GOVERNING EQUATIONS AND SYMMETRY

Let us consider a nematic layer filling the space $-d/2 < z < d/2$ bounded by infinite parallel plates, one of which (upper) oscillating harmonically along x with amplitude A and circular frequency $\omega = 2\pi f$. The director is oriented (rigidly anchored) at the boundaries along y , i.e., perpendicular to the flow plane. An electric field of strength E can be applied along z .

Before any instability develops (sufficiently small amplitude A) the director remains undistorted and the nematic behaves like an isotropic fluid with viscosity $\eta_3 = \alpha_4/2$. For further consideration let us introduce the dimensionless variables

$$\tilde{z} = z/d, \quad \tilde{t} = t\omega, \quad a = A/d.$$

In following we omit the tildes. Then the *subcritical* velocity profile can be found from Navier-Stokes equation

$$\epsilon_v^{-1} v_{x,t}^0 = v_{x,zz}^0, \quad v_x^0 \Big|_{z=1/2} = a \cos t, \quad v_x^0 \Big|_{z=-1/2} = 0. \quad (1)$$

Here $\epsilon_v = 1/(\omega\tau_v)$ with $\tau_v = \rho d^2/\eta_3$ the viscous relaxation time. Thus, our *basic* state is

$$\mathbf{n}^0 = (0, 1, 0), \quad \mathbf{v}^0 = [v_x^0(z, t), 0, 0]. \quad (2)$$

Below it will be shown that for the stability problem the inertia of fluid in the basic velocity field can be neglected, so that the solution of (1) is simply $v_x^0 = a(z + 1/2) \cos t$. In order to investigate the stability of (2) we linearize the nematodynamic equations [5] around this state

$$\begin{aligned} \mathbf{n} &= (0, 1, 0) + (n_x, n_y, n_z), \\ \mathbf{v} &= (v_x^0, 0, 0) + (v_x, v_y, v_z), \end{aligned}$$

where the perturbations $n_i = n_i(y, z, t)$, $v_i = v_i(y, z, t)$, $\{i = x, y, z\}$ are small. Here we neglect the x dependence of perturbations assuming the wave vector of instability if not zero is perpendicular to the shear direction.

Eliminating v_y by use of the incompressibility condition $v_{y,y} = -v_{z,z}$ and the pressure by cross differentiating the nematodynamic equations one obtains

$$\begin{aligned} (\epsilon_v^{-1} \hat{L}_1 + \hat{L}_2) v_x &= -\epsilon_v^{-1} \partial_{yy} v_z a \cos(t) + \alpha'_2 \partial_{yyy} t n_x + \\ &+ \frac{\alpha'_5 - \alpha'_2}{2} a \cos(t) \partial_{yyy} n_z; \end{aligned} \quad (3)$$

$$(\epsilon_v^{-1} \hat{L}_3 + \hat{L}_4) v_z = \hat{F}_1 n_z + a \cos(t) \hat{F}_2 n_x; \quad (4)$$

$$(\hat{G}_1 + \epsilon_d \hat{G}_2) n_x = (1 - \lambda)^{-1} [n_z a \cos(t) + v_{x,y}]; \quad (5)$$

$$(\hat{G}_3 + \epsilon_d \hat{G}_4) n_z = (1 - \lambda)^{-1} [\lambda n_{x,y} a \cos(t) + (\partial_{yy} - \lambda \partial_{zz}) v_z], \quad (6)$$

where \hat{L}_i , \hat{G}_i and \hat{F}_i are linear differential operators

$$\begin{aligned} \hat{L}_1 &= \partial_{yyt}, & \hat{L}_2 &= -(\eta'_2 \partial_y^4 + \partial_{zzyy}), \\ \hat{L}_3 &= \partial_{yyt} + \partial_{zzt}, & \hat{L}_4 &= -[\eta'_2 \partial_y^4 + (\alpha'_1 + \eta'_1 + \eta'_2) \partial_{zzyy} + \eta'_1 \partial_z^4], \\ \hat{F}_1 &= \alpha'_2 \partial_{yyy} - \alpha'_3 \partial_{zzyt}, & \hat{F}_2 &= \frac{\alpha'_6 - \alpha'_3}{2} \partial_y^3 - \frac{\alpha'_3 + \alpha'_6}{2} \partial_{yzz}, \\ \hat{G}_1 &= \partial_t, & \hat{G}_2 &= -(k_3 \partial_{yy} + k_2 \partial_{zz}), \\ \hat{G}_3 &= \partial_{yt}, & \hat{G}_4 &= -[k_3 \partial_y^3 + k_3 \operatorname{sgn}(\epsilon_a) \pi^2 E_0^2 \partial_y + \partial_{zzy}], \end{aligned}$$

and

$$\begin{aligned}\epsilon_d &= 1/(\tau_d \omega), \quad \tau_d = \gamma_1 d^2 / K_{11}, \quad E_0 = E/E_F, \\ \alpha'_i &= \alpha_i / \eta_3, \quad \eta'_i = \eta_i / \eta_3, \\ \gamma_1 &= \alpha_3 - \alpha_2, \quad \lambda = \alpha_3 / \alpha_2, \\ \eta_1 &= (\alpha_3 + \alpha_4 + \alpha_6) / 2, \quad \eta_2 = (\alpha_4 + \alpha_5 - \alpha_2) / 2.\end{aligned}$$

Here $k_i = K_{ii}/K_{11}$ with K_{ii} the orientation elastic constants, τ_d the director relaxation time, $E_F = \pi/d\sqrt{K_{11}/(\epsilon_0|\epsilon_a|)}$ the Fréedericksz field, ϵ_a the anisotropy of the dielectric permeativity. Notation $f_{,i} \equiv \partial f / \partial i$ has been used throughout. We introduce the quantity $P_\rho = \tau_v / \tau_d = \rho K_{11} / (\eta_3 \gamma_1)$, which is of order 10^{-6} for ordinary nematics.

The boundary conditions (*fully rigid*) read

$$\begin{aligned}v_x \Big|_{z=\pm 1/2} &= 0, \quad v_z \Big|_{z=\pm 1/2} = v_{z,z} \Big|_{z=\pm 1/2} = 0, \\ n_x \Big|_{z=\pm 1/2} &= 0, \quad n_z \Big|_{z=\pm 1/2} = 0.\end{aligned}\tag{7}$$

III. STABILITY ANALYSIS

A. General formulation

Let us collect all perturbations in the vector $\mathbf{Y} = (v_x, v_z, n_x, n_z)^T$. From the Floquet theorem one can write the model solutions of (3-6) in the form

$$\mathbf{Y} = e^{\sigma t} e^{iqy} \sum_{k=-\infty}^{\infty} \mathbf{y}_k(z) e^{kit},\tag{8}$$

where σ is the growth rate, q is a wave number of instability. Instead of solving the Floquet problem (8) directly we will employ a Galerkin expansion [19]:

$$\mathbf{y}_k = \sum_{n=1}^{\infty} \mathbf{c}_{nk} \phi_n(z),\tag{9}$$

where \mathbf{c}_{nk} are constant coefficients and $\phi_n(z)$ is a set of trial functions, which satisfy boundary conditions (7), Chebyshev functions [20]

$$\phi_n(z) = \begin{cases} T_{2m}(2z) - T_0(2z), & n = 2m - 1, \\ T_{2m+1}(2z) - T_1(2z), & n = 2m, \end{cases}\tag{10}$$

for v_x, n_x and n_z and Chadrasekhar functions [21]

$$\phi_n(z) = \begin{cases} \cosh(\lambda_m z) / \cosh(\lambda_m / 2) - \cos(\lambda_m z) / \cos(\lambda_m / 2), & n = 2m - 1, \\ \sinh(\nu_m z) / \sinh(\nu_m / 2) - \sin(\nu_m z) / \sin(\nu_m / 2), & n = 2m \end{cases}\tag{11}$$

for v_z . Here λ_m and ν_m are the roots of the appropriate characteristic equations [21].

Due to the structure of Eqs.(3-6) the model solutions (8)-(9) have the definite parity in z and t (parity of Fourier modes). Thus, the symmetry types are divided into four groups (Table I). The z -parity of v_y is opposite to that of v_z whereas the t -parity is the same. Type I corresponds to the Y -symmetry and type II to the Z -symmetry in the notations of PG [10]. Type I and III suppose that v_z can have nonzero time averaged and rolls in this case are *overturning*, i.e. they rotate steadily. Rolls of II and IV type are *oscillating*.

Substituting (8)-(9) into (3-6) and projecting [19] onto the Galerkin modes one obtains a linear algebraic system for the expansion coefficients \mathbf{c}_{nk} of the form

$$(\mathbf{A} + a\mathbf{B})\mathbf{c} = \sigma \mathbf{C}\mathbf{c}.\tag{12}$$

The expansions (8)-(9) are then truncated and the eigenvalue problem (12) can be solved. The condition $\Re[\sigma(a, q)] = 0$ for the largest sigma yields the neutral curve $a_0(q)$. If one assumes a stationary bifurcation, i.e. $\Im(\sigma) = 0$ at the threshold, then one has to solve the eigenvalue problem

$$(\mathbf{A}^{-1}\mathbf{B})\mathbf{c} = -\frac{1}{a}\mathbf{c}, \quad (13)$$

which is much more convenient. The critical value a_c is given by $a_c = \min_q a_0(q)$, which also yields the critical wave number q_c . Using (12) we have checked that the first bifurcation is really always stationary [22].

B. Results without electric field

The calculations were done for material MBBA, see App. C for material parameters.

For $\omega\tau_d \leq 35$ the first instability developing in the absence of external fields is a homogeneous one ($q_c = 0$) [10]. This could be expected already from the fact that in steady shear flow the homogeneous instability occurs first [10]. At $\omega\tau_d \sim 35$ PG have observed the transition to rolls of type I. Up to now the frequency region $\omega\tau_d > 35$ remains experimentally poorly investigated. Our analysis for $\omega\tau_d \geq 35$ shows that roll instability of type I persists up to $\omega\tau_d \sim 4.1 \cdot 10^4$, where a transition to the rolls of II-type takes place (Fig.1). At the transition point the wave number jumps from 12 to 1.2. We have checked numerically that the appearance of this transition is related to the inertia of the nematic described by the parameter ϵ_v . By neglecting the inertia term in the Navier-Stokes Eqs. (3-4), i.e. for $\epsilon_v^{-1} \rightarrow 0$, no such transition was found. Numerical analysis also shows that thresholds for instabilities of III and IV types are higher for all frequencies investigated.

In order to understand the mechanism leading to this transition let us analyze Eqs.(3)-(6). By acting with ∂_y on Eq. (3) and with $\partial_{yy} - \lambda\partial_{zz}$ on (4) one may eliminate the velocities. In the remaining equations for n_x and n_z we use a one-mode spatial approximation

$$\begin{aligned} n_x &= \cos(\pi z) \cos(qy) f(t), \\ n_z &= \cos(\pi z) \cos(qy) g(t), \end{aligned}$$

appropriate for the symmetry of type I or II. Projecting the equations one obtains coupled second order ODEs for $f(t)$ and $g(t)$. Further simplifications can be made by neglecting the terms proportional to P_ρ and ϵ_v^{-3} . One then arrives at

$$\dot{f} + \epsilon_d m_1 f + (\epsilon_v^{-1} m_3 a \sin t - m_2 a \cos t) g = 0, \quad (14)$$

$$\dot{g} + \epsilon_d l_1 g - l_2 a \cos t f = 0. \quad (15)$$

Coefficients $m_i(q), l_i(q)$ are presented in Appendix A. In looking for expressions for the critical amplitude we assume

$$\begin{aligned} f &= f_{osc}, & g &= g_{st} + g_{osc} & \text{for type I,} \\ f &= f_{st} + f_{osc}, & g &= g_{osc} & \text{for type II,} \end{aligned} \quad (16)$$

that corresponds to the separation of the functions f and g into the stationary (index *st*) and oscillatory (*osc*) parts. Substituting (16) into (14)-(15) and using time averaging procedure one obtains the critical amplitudes for roll instabilities of I and II type

$$\begin{aligned} a_c^I &= \left[2 \frac{(\epsilon_d^2 m_1^2 + 1)}{[m_1 m_2 + (\epsilon_v \epsilon_d)^{-1} m_3]} \frac{l_1}{l_2} \right]^{1/2}, \\ a_c^{II} &= \left[2 \frac{(\epsilon_d^2 l_1^2 + 1)}{[m_2 l_1 - (\epsilon_v \epsilon_d)^{-1} m_3]} \frac{m_1}{l_2} \right]^{1/2}. \end{aligned} \quad (17)$$

Let us analyze the formulas (17). From (A1) one has that $l_2(q)$ is positive for large q (> 2) and very small q ($\ll 1$). Taking into account that $l_1(q)$ is positive for all q and the expression $[m_1 m_2 + m_3 (\epsilon_v \epsilon_d)^{-1}]$ remains positive up to very large value of $\omega\tau_d$ ($\sim 10^6$) one sees from first Eq.(17) that in order to have a threshold l_2 has to be positive. Thus, only large q (rolls) and homogeneous instabilities can develop with symmetry of I type. In the second Eq.(17) the expression $[m_2 l_1 - m_3 (\epsilon_v \epsilon_d)^{-1}]$ in the denominator changes sign with increasing frequency from positive to negative at the frequency given by

$$(\omega\tau_d)_{tr}^2 = \frac{m_2 l_1}{m_3} \frac{1}{P_\rho}, \quad (18)$$

A lower limit of the transition frequency is given by setting $q = 0$ in (18). Below $(\omega\tau_d)_{tr}$ one has $[m_2l_1 - m_3(\epsilon_v\epsilon_d)^{-1}] > 0$. Since $m_1 > 0$ for all q one needs $l_2 > 0$ to have a threshold, i.e., only the large q instability (rolls) can exist. For $\omega\tau_d > (\omega\tau_d)_{tr}$ one needs negative l_2 , which provides an instability with small q . One can conclude from (17) that only the product $\epsilon_v\epsilon_d$ plays an essential role in the transition from rolls of I type symmetry to rolls of II type, not ϵ_v itself.

Let us now return to the question of neglecting the inertia term in Eq.(1) for the basic velocity. Assuming ϵ_v^{-1} to be small (for $\omega\tau_d \ll 1/P_\rho \sim 10^6$) one can find the expression for basic velocity v_x^0 as an expansion in ϵ_v^{-1} . Keeping only the first correction changes the threshold amplitude [and, consequently, $(\omega\tau_d)_{tr}$] by less than 1%, so that ϵ_v^{-1} can really be neglected in (1).

The results for the approximate expressions (17) are included in Fig.1. The formulas (17) have an error of about 30% at small $\omega\tau_d$, which grows further with $\omega\tau_d$. This is an obvious consequence of the one-mode approximation. Nevertheless, the analytic expressions show all the important features of the numerically calculated thresholds, including the switching between the modes of I and II types. However, one should note that the frequency dependence of the critical wave number q_c in the one-mode approximation does for I type rolls not show the saturation like in the numerical calculations.

For $\omega\tau_d \gg 1/\sqrt{P_\rho}$, when $1/(\epsilon_v\epsilon_d) \gg 1$, one can expand Eqs. (17) in $1/(\epsilon_v\epsilon_d)$. For the threshold of II type rolls one gets

$$a_c^{II} = \left[-2 \frac{(\epsilon_d^2 l_1^2 + 1)}{m_2 l_1} \frac{m_1}{l_2} P_\rho \right]^{1/2} \frac{1}{\omega\tau_d}. \quad (19)$$

Since $\epsilon_d \ll 1$ for $\omega\tau_d \gg 1$ one can see that a_c^{II} is inversely proportional to $\omega\tau_d$.

By increasing $\omega\tau_d$ the critical amplitude $a_c(\omega\tau_d)$ of mode I appears to tend to a constant value already at rather low $\omega\tau_d$, where $\epsilon_v^{-1} \ll 1$. Such behavior was found in [24] by an one-mode analysis. One can show that this feature is not a artefact of the one-time-mode approximation. The same result can be obtained by inspection of the high-frequency limit in (14)-(15) (see Appendix B).

Summarizing, we conclude from our analysis that increasing of the oscillatory flow frequency (for given cell thickness d) leads to switching from I to II symmetry type roll instability. It has been shown that this transition is caused by the inertia of the nematic fluid described by the parameter ϵ_v^{-1} . For MBBA material parameters one has the transition at $\omega\tau_d \sim 4.1 \cdot 10^4$. Consequently, in the PG experiment [10] with the same liquid crystal and $d = 240 \mu\text{m}$ the transition frequency should occur of about 7 Hz (maximal frequency in this experiment was ~ 2 Hz). Recent experiments [12], [13] show that this transition could be observed.

C. Comparison with experiments

Experiments of Mullin and Peacock (MP) [12] performed with the nematic E7 show the existence of a roll instability at least up to 160 Hz with d between 20 and $50 \mu\text{m}$. MP report, that the observation of probe particle have not shown any macroscopic flow, which could mean that the rolls are of II, i.e., the oscillating type. We have found in the literature only the values of the elastic constants for E7 [23], so that we are not able to perform a direct comparison of our theoretical results with the MP experimental data. One can consider the influence of material parameters variation on the instability type. The results of this consideration are presented in table II. A good test for the quality of oscillatory Couette flow realized in experiments is scaling law, which says, that $A/d = F(\omega\tau_d^2)$, where F is some function to be determined from nematodynamic equations. The experimental data of MP [12] satisfy this test only in a rather narrow region of low frequencies, namely, up to about 40 Hz. At higher frequencies the scaling law becomes broken, which could be caused by failure of surface anchoring.

Oscillatory shear flow was investigated experimentally also by Anikeev and Kapustina [13]. The authors used an eutectic mixture of MBBA and EBBA, which is known to have almost the same material parameters as MBBA. A geometry where the director is anchored in the plane of the layer at an angle ψ to the shear direction was investigated. For the case $\psi = 90^\circ$, which we are interested in, the frequency dependence of a_c and q_c are presented. The experimental points taken from [13] are given in Fig.1 together with theoretical curves. The agreement between experimental and theoretical data is good.

D. Influence of electric field on the instability type and symmetry

Applying an electric field across the nematic layer can lead to the switching in particular between the different types of temporal symmetry of rolls induced by oscillatory shear flow. In the case of MBBA a change of the roll instability

of I type to II type by increasing the electric field strength was observed [10]. We performed the stability analysis of the linearized equations (3)-(6) in a wide range of oscillatory flow frequency and electric field strength for MBBA, which has a *negative* anisotropy of the dielectric permeativity. We have found that the electric field can change not only the temporal symmetry of instability, but also the spatial one. The phase diagram (Fig. 2) presents the area, where the rolls with symmetry type III appear at threshold. According to their spatial symmetry these rolls represent a double-layered structure, so that the critical wave number in this area is about two times larger than otherwise. For low values of $\omega\tau_d$ an applied electric field leads to an increase of the area of homogeneous instability (*HI*), so that the electric field suppress the roll instability. The profiles of the velocity and the director in the various modes are plotted in Fig. 3.

We have also calculated the phase diagram for a nematic with *positive* dielectric anisotropy (Fig.4). The material parameters were taken from MBBA except for setting the dielectric anisotropy to be positive. In this case the phase diagram (Fig.4) presents an extensive area of rolls of II symmetry type. At low $\omega\tau_d$ there is a switching between homogeneous instabilities of I and II types by varying the electric field. Note, that under these conditions Fréedericksz transition takes place at voltage U_F (~ 3.74 V). As a result, when U approaches U_F , the critical shear amplitude a_c goes to zero.

The one-mode analysis in this case gives unsatisfactory agreement with the full numerical calculations, although it keeps all the important features (switching between modes *etc.*).

IV. DISCUSSION AND CONCLUSION

We obtained the complete phase diagram of the orientational instabilities, both homogeneous and spatially periodic, in nematic liquid crystal subjected to oscillatory Couette flow based on the linear stability analysis of the full set of nematodynamic equations. It has been found for the first time that the inertia of nematic fluid, usually neglected in the theoretical considerations, is responsible for the new type of roll instability and switching between roll instabilities with different time-symmetry. The results of approximate analytical analysis show an essential features of the influence of inertia of nematic fluid on the instability scenarios and are in a good agreement with full numerical simulations of underlying equations. For the nematic liquid crystal MBBA increasing of flow frequency leads to the transition between rolls of I and II symmetry types.

Both these modes can be easily distinguished in the experiments. Although there are no reports concerning the observations of this transition, the recent experiments on oscillatory flow in nematics show that the technical possibilities are rich enough to observe such effect.

We have also investigated the influence of additional electric field applied across the nematic layer on the flow instabilities for the liquid crystals with negative and positive dielectric anisotropy. In case of MBBA it was found that the electric field causes transition to the double-layered roll structure, which is intermediate regime between rolls of I and II types observed in [10]. Another interesting point in the experimental investigations could be the transition between rolls of the same symmetry but quite different wave numbers at increasing of flow frequency (RII_1 and RII_2 in Fig.2).

ACKNOWLEDGMENTS

We wish to thank T. Mullin and T. Peacock for communicating us results before publication. O.T. thanks the Deutscher Akademischer Austauschdienst (DAAD) for financial support. Work supported by Deutsche Forschungsgemeinschaft Grants No. Kr 690/12, Kr 690/14 and INTAS Grant No. 96-498.

APPENDIX A: COEFFICIENTS

Coefficients for (14)-(15) are

$$\begin{aligned}
 m_1 &= (\pi^2 k_2 + q^2 k_3)(q^2 \eta'_2 + \pi^2)/r_1, \\
 m_2 &= (1 - \lambda)^{-1} [q^2(\eta'_2 - \frac{\alpha'_5 - \alpha'_2}{2}) + \pi^2]/r_1, \\
 m_3 &= (1 - \lambda)^{-1}/r_1, \\
 l_1 &= r_2[\pi^2 + k_3(q^2 - \text{sgn}(\epsilon_a)\pi^2 E_0^2)]/r_3, \\
 l_2 &= (1 - \lambda)^{-1} [\lambda r_2 - \frac{\alpha'_6 - \alpha'_3}{2} + \\
 &\quad + q^2 \pi^2 (\frac{\alpha'_6 - \alpha'_3}{2} + \frac{\alpha'_3 + \alpha'_6}{2}) - \pi^4 \lambda \frac{\alpha'_3 + \alpha'_6}{2}]/r_3,
 \end{aligned} \tag{A1}$$

with

$$\begin{aligned} r_1 &= q^2(\eta'_2 + (1 - \lambda)^{-1}\alpha'_2) + \pi^2, \\ r_2 &= q^2[\pi^2(\alpha'_1 + \eta'_1 + \eta'_2) + q^2\eta'_2] + \pi^4\eta'_1, \\ r_3 &= r_2 + (1 - \lambda)^{-1}[q^4\alpha'_2 - q^2\pi^2(\lambda\alpha'_2 + \alpha'_3) + \pi^4\lambda\alpha'_3]. \end{aligned}$$

APPENDIX B: HIGH-FREQUENCY LIMIT

To investigate the behavior of the critical amplitude in the high-frequency range we neglect ϵ_v^{-1} in (14) and (15) and expand the functions f and g in small parameter $\epsilon_d = 1/(\omega\tau_d)$. Formally this analysis is valid for $1 \ll \omega\tau_d \ll 1/P_\rho$ (for MBBA material parameters and $d = 20 \mu\text{m}$ this corresponds to $0.02 \text{ Hz} \ll f \ll 10^6 \text{ Hz}$).

Setting $\epsilon_v^{-1} = 0$ in (14)-(15) one has in matrix form

$$\frac{d}{dt}\mathbf{Y} = \mathbf{A}(t)\mathbf{Y}, \quad (\text{B1})$$

where

$$\mathbf{Y} = \begin{pmatrix} f \\ g \end{pmatrix}, \quad \mathbf{A} = \begin{pmatrix} -\epsilon_d m_1 & -m_2 a \cos t \\ -l_2 a \cos t & -\epsilon_d l_1 \end{pmatrix}.$$

We seek periodic solution of (B1) of the form

$$\mathbf{Y} = \mathbf{Y}_0 + \epsilon_d \mathbf{Y}_1 + \dots$$

At order in ϵ_d^0 one has

$$\frac{d}{dt}\mathbf{Y}_0 = \mathbf{A}_0(t)\mathbf{Y}_0 \quad (\text{B2})$$

where $\mathbf{A}_0 = \mathbf{A}\Big|_{\epsilon_d=0}$. Since $\mathbf{A}_0(t)$ commutes with $\mathbf{A}_0(t')$ (unlike \mathbf{A}) the solution of (B2) has a form

$$\mathbf{Y}_0 = e^{\int_0^t d\tau \mathbf{A}_0(\tau)} \mathbf{Y}^0, \quad \mathbf{Y}^0 = \begin{pmatrix} f^0 \\ g^0 \end{pmatrix}, \quad (\text{B3})$$

where f^0 and g^0 are initial values (fluctuations) of the functions f_0 and g_0 , respectively. It can be easily seen, that \mathbf{Y}_0 is periodic with time averages $\langle f_0 \rangle_t \sim f^0$, $\langle g_0 \rangle_t \sim g^0$, so that the state with $(f^0 = 0, g^0 \neq 0)$ corresponds to the mode of I symmetry type, the state $(f^0 \neq 0, g^0 = 0)$ corresponds to mode of II symmetry type. At first order in ϵ_d one has the system

$$\frac{d\mathbf{Y}_1}{dt} = \mathbf{A}_0(t)\mathbf{Y}_1 + \mathbf{b}, \quad \text{with} \quad \mathbf{b} = \begin{pmatrix} -m_1 f_0 \\ -l_1 g_0 \end{pmatrix} \quad (\text{B4})$$

The solution of (B4) is given by

$$\mathbf{Y}_1 = \mathbf{Y}_0 + e^{\int_0^t d\tau \mathbf{A}_0(\tau)} \int_0^t d\tau e^{-\int_0^\tau d\xi \mathbf{A}_0(\xi)} \mathbf{b}(\tau). \quad (\text{B5})$$

Substituting expressions for \mathbf{b} into (B5) and using the relation [20]

$$\begin{aligned} e^{z \sin \theta} &= I_0(z) + 2 \sum_{k=0}^{\infty} (-1)^k I_{2k+1}(z) \sin(2k+1)\theta + \\ &\quad 2 \sum_{k=0}^{\infty} (-1)^k I_{2k}(z) \cos 2k\theta, \end{aligned}$$

where I_i are modified Bessel functions of the first kind, one has the periodicity condition of \mathbf{Y}_1

$$I_0(2\sqrt{m_2 l_2} a) = -\frac{l_1 + m_1}{l_1 - m_1} \quad \text{for I type,} \quad (B6)$$

$$I_0(2\sqrt{m_2 l_2} a) = \frac{l_1 + m_1}{l_1 - m_1} \quad \text{for II type.} \quad (B7)$$

Eqs. (B6) and (B7) represent the connection between a and q in implicit form, i.e. the neutral curve $a_0(q)$. Minimizing $a_0(q)$ gives the critical values of the flow amplitudes a_c and the wave number q_c . Equation (B7) has no real roots for $q > 0.5$, so that when the fluid inertia term is neglected only a roll instability of I symmetry type or homogeneous instability of II symmetry type can appear. Eq. (B6) gives a critical amplitude $a_c \sim 2.2$ and wave number $q_c \sim 12$ and for , that is in a good agreement with numerical results (Fig.1). From (B7) it follows that the smallest threshold $a_c = 10.9$ corresponds to $q_c = 0$.

The above analysis shows the role of the elasticity described by terms proportional to ϵ_d in the nematodynamic equations. The nature of these terms is singular, i.e. when neglecting these terms the critical flow amplitude vanishes ($a_c = 0$), although for infinitesimal ϵ_d there exists a finite value of a_c . Another point is that at high enough frequencies a_c does not depend on the flow frequency, which is in contrast to the case of director alignment in the flow plane [3], where the critical amplitude of roll formation under oscillatory shear flow decreases with increasing flow frequency.

APPENDIX C: MATERIAL PARAMETERS

The following values of the MBBA material parameters at 25 °C [25,26]:

$$K_{11} = 6.66, K_{22} = 4.2, K_{33} = 8.61 \quad (\text{in units } 10^{-12} \text{ N});$$

$$\alpha_1 = -18.1, \alpha_2 = -110.4, \alpha_3 = -1.1, \alpha_4 = 82.6, \alpha_5 = 77.9, \alpha_6 = -33.6 \quad (\text{in units } 10^{-3} \text{ N}\cdot\text{s/m}^2).$$

$$\epsilon_a = -0.53.$$

$$\text{Fréedericksz transition voltage is defined by } U_F = \pi \sqrt{\frac{K_{11}}{\epsilon_0 |\epsilon_a|}}.$$

- [1] P.G. de Gennes, *The Physics of Liquid Crystals* (Clarendon Press, Oxford, 1974).
- [2] E. Dubois-Violette P. and Manneville, in *Pattern Formation in Liquid Crystals*, edited by A. Buka and L. Kramer, (Springer-Verlag, New York, 1996), Chap. 4, p. 91.
- [3] A.P. Krekhov, T. Börzsönyi, P.Tóth, A. Buka and L. Kramer, *Phys. Rep.*, **337**, 171 (2000).
- [4] I. Zuniga and F.M. Leslie, *Liq. Cryst.*, **5**, 725 (1989).
- [5] F.M. Leslie, *Adv. Liq. Cryst.*, **4**, 713 (1979).
- [6] S.A. Pikin, *JETP*, **31**, 176 (1974).
- [7] S.A. Pikin and V.G. Chigrinov, *JETP*, **31**, 176 (1974).
- [8] A.P. Krekhov and L. Kramer, *Phys. Rev. E*, **53**, 4925 (1996).
A. P. Krekhov and L. Kramer, *J. de Phys. II (France)*, **4**, 677 (1994).
- [9] O.S. Tarasov and A.P. Krekhov, *Cryst. Rep.*, **44**, 1121 (1999).
- [10] P. Pieranski and E. Guyon, *Phys. Rev. A*, **9**, 404 (1974).
- [11] E. Guyon and P. Pieranski, *J. de Phys. (France)*, **36**, C1-203 (1975).
- [12] T. Mullin and T. Peacock, *Proc. Roy. Soc. Lon. A*, **455**, 2635 (1999).
- [13] D.I. Anikeev and O.A. Kapustina, *JETP*, **83**, 731 (1996).
- [14] E. Dubois-Violette, E. Guyon, I. Janossy, P. Pieranski and P. Manneville, *J. de Mec.*, **16**, 733 (1977).
- [15] P. Manneville and E. Dubois-Violette, *J. de Phys. (France)*, **37**, 285 (1976).
- [16] P. Manneville and E. Dubois-Violette, *J. de Phys. (France)*, **37**, 1115 (1976).
- [17] I. Janossy, P. Pieranski and E. Guyon, *J. de Phys. (France)*, **37**, 1105 (1976).
- [18] P. Manneville, *J. de Phys. (France)*, **40**, 713 (1979).
- [19] D. Gottlieb and S.A. Orszag, *Numerical analysis of spectral methods: theory and applications* (Montpellier: Capital City Press, 1993)
- [20] M. Abramowitz and I.A. Stegun, *Handbook of Mathematical Functions* (New York:Dover, 1964).
- [21] S. Chandrasekhar, *Hydrodynamic and Hydromagnetic stability*, (Oxford University Press, 1961).
- [22] Indeed, there is known numerical effect: periodical force provides the existence of parasitic eigenvalues in (12), which have non-zero real parts at the threshold amplitude corresponding to the stationary bifurcation. The imaginary parts of these eigenvalues are integer numbers, so that the parasitic eigenvalues are easily to be found and eliminated.
- [23] F. Yang, J.R. Sambles and G.W. Bradberry, *J. Appl. Phys.*, **85**, 728 (1999).
F. Yang, J.R. Sambles, Y. Dong and H. Gao, *J. Appl. Phys.*, **87**, 2726 (2000).

[24] E. Dubois-Violette, E. Guyon, I. Janossy, P. Pieranski and P. Manneville, *J. de Mec.*, **16**, 733 (1977).
 [25] W.H. de Jeu, W.A.P. Claassen and A.M.J. Spruijt, *Mol. Cryst. Liq. Cryst.*, **37**, 269 (1976).
 [26] H. Knepp, F. Schneider and N.K. Sharma, *J. Chem. Phys.*, **77**, 3203 (1982).

	I		II		III		IV	
	z	t	z	t	z	t	z	t
v_x	even	odd	even	even	odd	odd	odd	even
v_z	even	even	even	odd	odd	even	odd	odd
n_x	even	odd	even	even	odd	odd	odd	even
n_z	even	even	even	odd	odd	even	odd	odd

TABLE I. Spatial (z) and temporal (t) symmetries of solutions of linearized equations (3)-(6).

	Standard values	Transition values	New a_c	New q_c
α_1/α_2	0.164	1.01	2.38	6.9
α_4/α_2	-0.748	-5.92	7.72	10.1
α_5/α_2	-0.706	-1.83	6.64	1.4
α_6/α_2	0.304	-0.85	6.60	1.4
K_{11}/K_{22}	1.586	5.95	2.93	7.3
K_{33}/K_{22}	2.05	0.15	1.66	16.6

TABLE II. In the second column the normalized standard values for the material parameters of MBBA at $25^\circ C$ are given. With those values and at $\omega\tau_d = 825$ (typical value for experiment [12]) the roll instability of I type (overturning rolls) takes place with critical amplitude $a_c = 2.6$ and critical wave number $q_c = 7$. When any one of the parameters is varied alone a transition to II type rolls (oscillating ones) occurs at the value in the third column. In the fourth and fifth columns the new values of the threshold amplitude and the critical wave number are given.

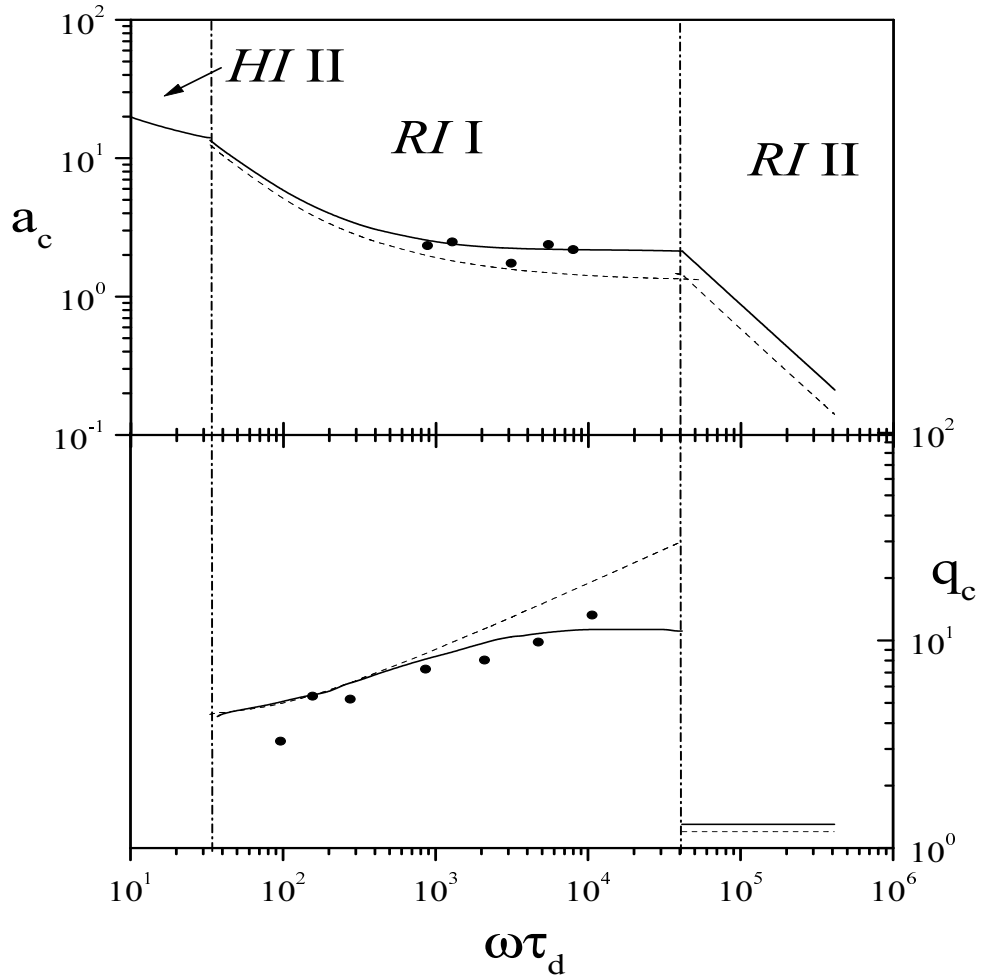


FIG. 1. Critical amplitude a_c vs. $\omega\tau_d$ for MBBA. Solid lines are numerical calculations, dashed lines are approximations (17), points are experimental data from [13]. *RI* denotes roll instability, *HI* is homogeneous instability, Roman numbers denote the group of symmetry from table I.

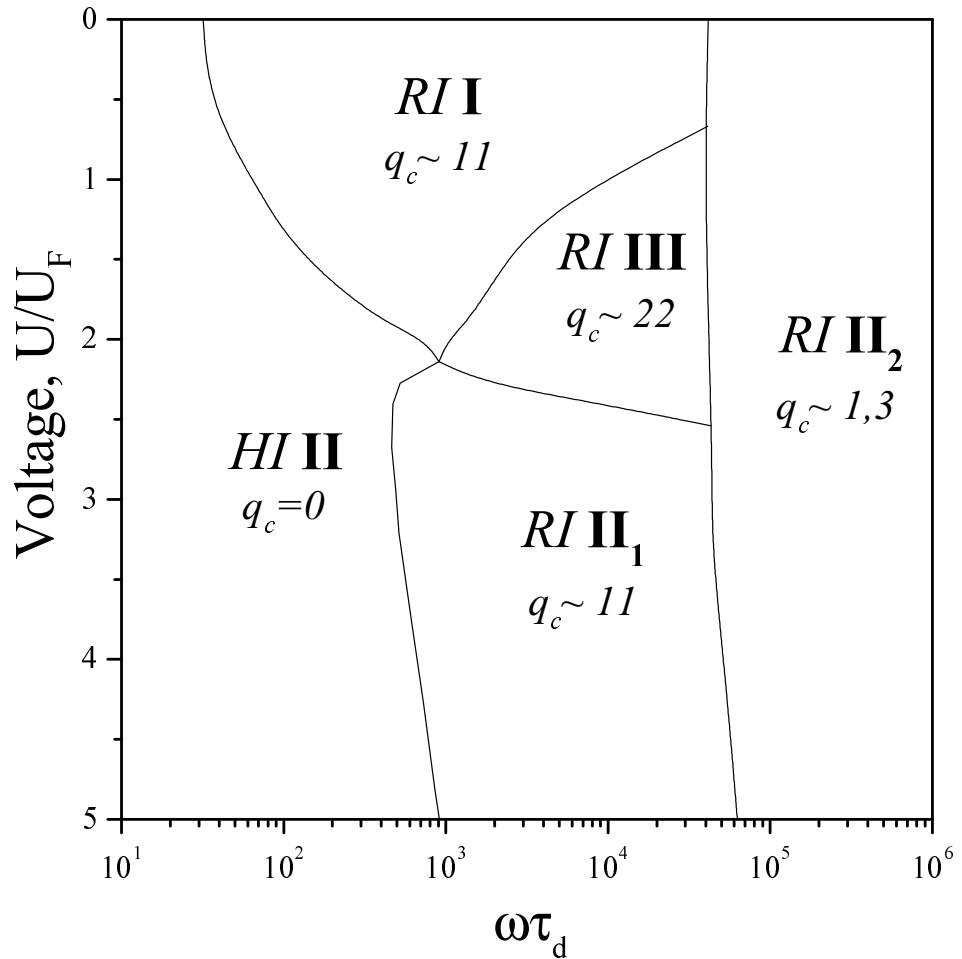


FIG. 2. Phase diagram of instabilities induced by oscillatory shear flow and affected by electric field a nematic with *negative* dielectric anisotropy. *RI* denotes roll instability, *HI* is homogeneous instability, Roman numbers denote the group of symmetry from table I.

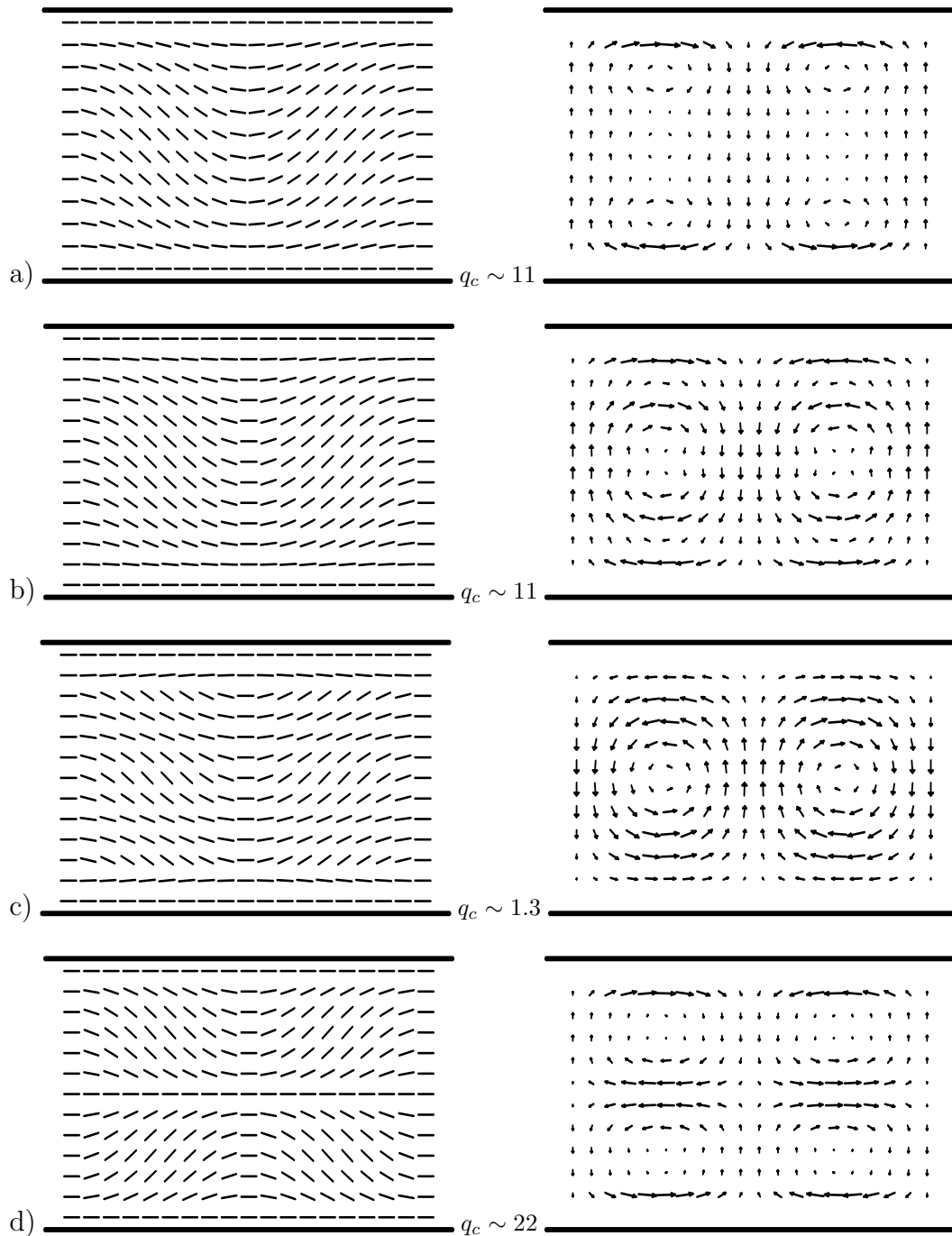


FIG. 3. Director (left) and velocity (right) profiles:
a) RII , time averaged,
b) RII_1 , $t = 0$,
c) RII_2 , $t = 0$,
d) $RIII$, time averaged.

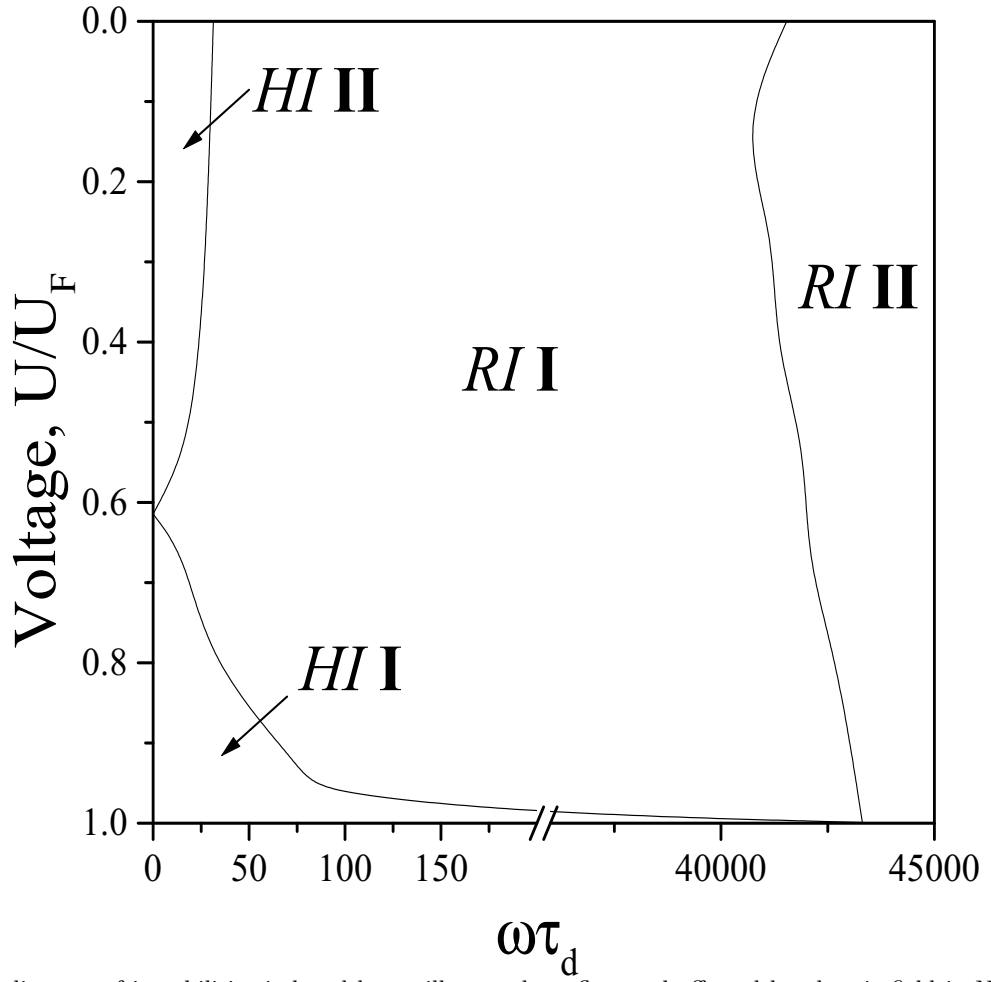


FIG. 4. Phase diagram of instabilities induced by oscillatory shear flow and affected by electric field in NLC with *positive* dielectric anisotropy. U_F is Fréedericksz transition voltage. RI denotes roll instability, HI is homogeneous instability, Roman numbers denote the group of symmetry from table I.